

## Supporting Information

### Turning conductive carbon nanospheres to nanosheets for high-performance supercapacitors of MnO<sub>2</sub> nanorods

Nutthaphon Phattharasupakun,<sup>a</sup> Juthaporn Wutthiprom,<sup>a</sup> Poramane Chiochan,<sup>a</sup> Phansiri Suktha,<sup>a</sup> Montakan Suksomboon,<sup>a</sup> Saran Kalasina,<sup>a</sup> and Montree Sawangphruk<sup>a</sup>

<sup>a</sup> Department of Chemical and Biomolecular Engineering, School of Energy Science and Engineering, Vidyasirimedhi Institute of Science and Technology, Rayong 21210, Thailand

\*Corresponding author. Tel: +66(0)33-01-4251 Fax: +66(0)33-01-4445.

E-mail address: montree.s@vistec.ac.th (M. Sawangphruk).

#### 1. Experimental

##### 1.1 Preparation of *f*-CFP

CFP (SGL CARBON SE, Germany) was stirred in a mixture of concentrated sulfuric acid (H<sub>2</sub>SO<sub>4</sub> 98%, QRec) and concentrated nitric acid (HNO<sub>3</sub> 65%, QRec) at a volume ratio of 3:1 at 60°C for 1 h. After the acid oxidation, the treated CFP was washed by deionized water several times and dried at 60°C for 24 h. After that, the *f*-CFP was obtained and then cut in diameter of 0.79 cm for using as the working electrode or substrate for the supercapacitors.

##### 1.2 Preparation of oxidized carbon nanoparticle

Oxidized carbon nanoparticle (OCN) was synthesized from black carbon nanoparticle (CN) by an acid oxidation method in a reflux condenser. For the synthesis of OCN, 5 g of CN was mixed with 400 ml of nitric acid (HNO<sub>3</sub> 65%,

QRec) in a 2-L round-bottom flask, the mixture was refluxed at 100 °C for 96 h. For purification, the suspension was washed with deionized water several times. The diluted suspension was centrifuged at 6000 rpm for 10 min, then filtered by using deionized water and ethanol. Finally, the OCB was collected in the form of black powder by vacuum dried at 60°C overnight.

### *1.3 Fabrication of symmetric supercapacitor device*

The fabrication of working electrode was carried out as follows. Manganese dioxide powder ( $\text{MnO}_2 \geq 90\%$ , Sigma-Aldrich), CN or OCN, and PVDF (Sigma-Aldrich) were mixed in different mass ratios (9:0:1, 8.5:0.5:1, 8:1:1, 7:2:1, 6:3:1, 5:4:1, and 4:5:1) in N-Methylpyrrolidone (NMP, QRec) solvent and then sonicated for 30 min. The homogeneous black solution was obtained and then coated on carboxyl-functionalized carbon fiber paper (f-CFP) by a spray-coating technique under pressure of 30 psi. The loading mass of  $\text{MnO}_2/\text{CN}/\text{PVDF}$  on each electrode was about 2 mg. The electrodes was inserted in the coin case (CR2016). Cellulose paper (No.5) was soaked in 0.5 M  $\text{Na}_2\text{SO}_4$  for 10 min and inserted between the electrodes as an electrolyte separator. Then CR2016 was pressurized at 800 psi for 10 s in a hydraulic press.

## **2. Calculation**

The specific capacitance (C) from the CV curves can be calculated by the following equation:

$$C_{cell, CV} = \frac{Q}{\Delta V_{CV} \times m_{cell}} \quad (1)$$

Where Q is an average charge in the discharge process (Coulomb) of CV curve,  $\Delta V_{CV}$  is the working potential window (V),  $m_{cell}$  is the mass of both active materials used in the positive and negative electrodes.

The SC from GCD cycling can be calculated by using the following equation:

$$C_{cell,GCD} = \frac{I_{GCD} \times \Delta t_{GCD}}{\Delta V_{GCD} \times m_{cell}} \quad (2)$$

Where  $I_{GCD}$  is the applied current (A) when discharging the supercapacitor cell by GCD,  $\Delta t_{GCD}$  is the discharge time of the cell (s),  $\Delta V_{GCD}$  is the working potential window (V) of the cell excluding the IR drop.

The SC from EIS can be calculated by using the following equation:

$$C_{cell,EIS} = \frac{-1}{2\pi f Z'' m_{cell}} \quad (3)$$

Where  $f$  is the applied frequency (Hz),  $Z''$  is the imaginary component at the frequency  $f$ .

The calculated specific capacitance mentioned in this work is based on a single electrode

$$C_s = 4C_{cell} \quad (4)$$

The Energy density and Power density can be calculated by the following equation.

$$E = \frac{1}{2} \times C_{cell} \times (\Delta V^2) \quad (5)$$

$$P = \frac{V_0^2}{4R_{cell}} \quad (6)$$

Where  $V_0$  is an initial voltage of the cell,  $R_{cell}$  is the cell's resistance in GCD.

### 3. FESEM image of MnO<sub>2</sub> nanorods

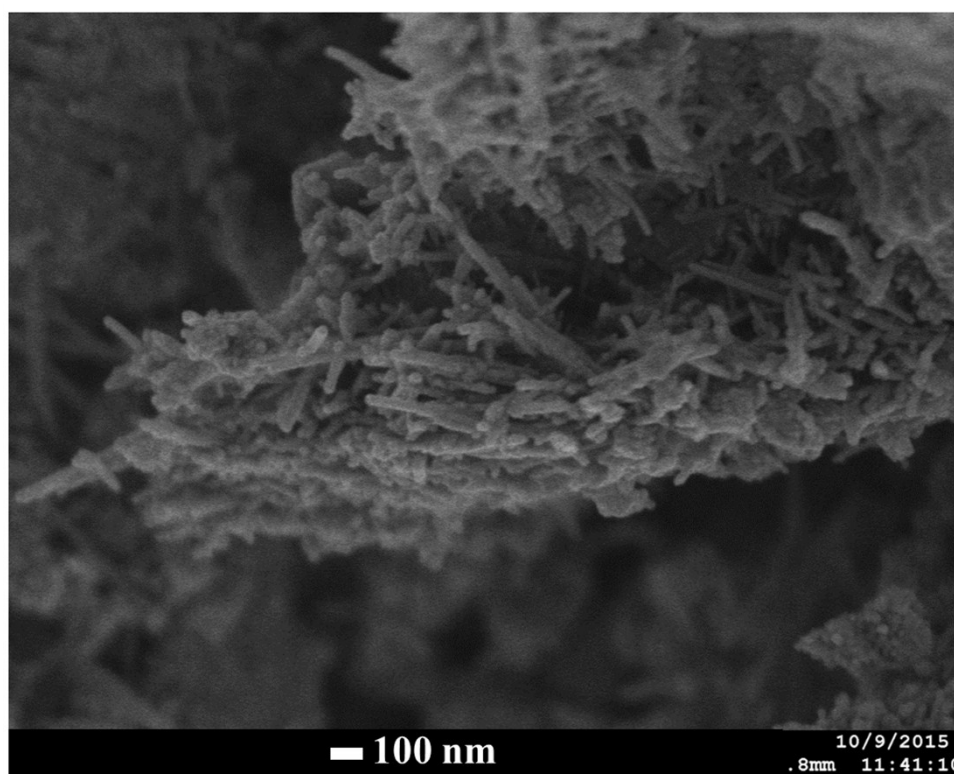


**Fig. S1.** FE-SEM image of MnO<sub>2</sub> nanorods marketed from Sigma Aldrich.

#### **4. XPS spectra of black carbon nanospheres (CN) and oxidized carbon nanosheets (OCN)**

Fig.S2a shows survey-scan XPS spectra of OCN and CN confirming the existence of oxygen functional group (O 1s) found on the surface of the OCN. The atomic O/C ratio of OCN is 0.1352, which is significantly higher than 0.004 of CN. The C 1s spectra of CN in Fig.S2b shows the sharp peak at 285.01 eV, which belongs to  $\text{-C=C-}$  and a very small amount of oxygen functional groups i.e., C-O (at 285.27 eV) and C-O-C (at 286.61 eV) due to the adsorbed oxygen-containing species. The  $\pi\text{-}\pi^*$  at 291.10 eV relates to the benzene ring network in the surface of black carbon nanospheres. After the oxidation process, Fig.S2c shows a C1s XPS spectrum of OCN for which the peaks of the oxygen species can clearly be observed owing to the oxygen-containing groups chemically bonded to the carbon nanosheets. Fig.S2d shows the narrow-scan O1s spectrum of OCN, which is deconvoluted to three peaks of O=C-OH (at 530.63 eV), C=O (at 532.16 eV), and C-OH (at 533.78 eV). This result can confirm the successful oxidation process.

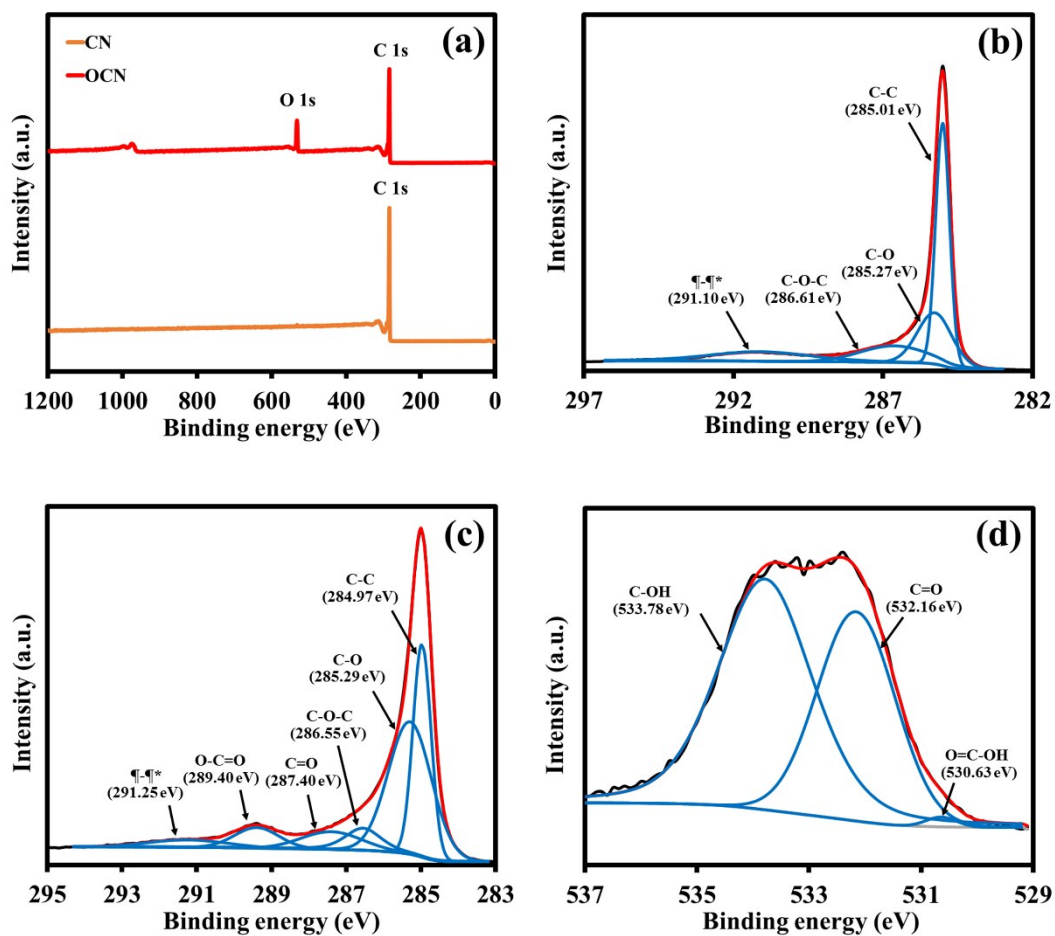


**Fig. S2.** (a) Wide-scan XPS spectra of OCN and CN, (b) narrow-scan C1s XPS spectrum of CN, and (c) narrow-scan C1s XPS spectrum of OCN, and (d) narrow-scan O1s XPS spectrum of OCN.

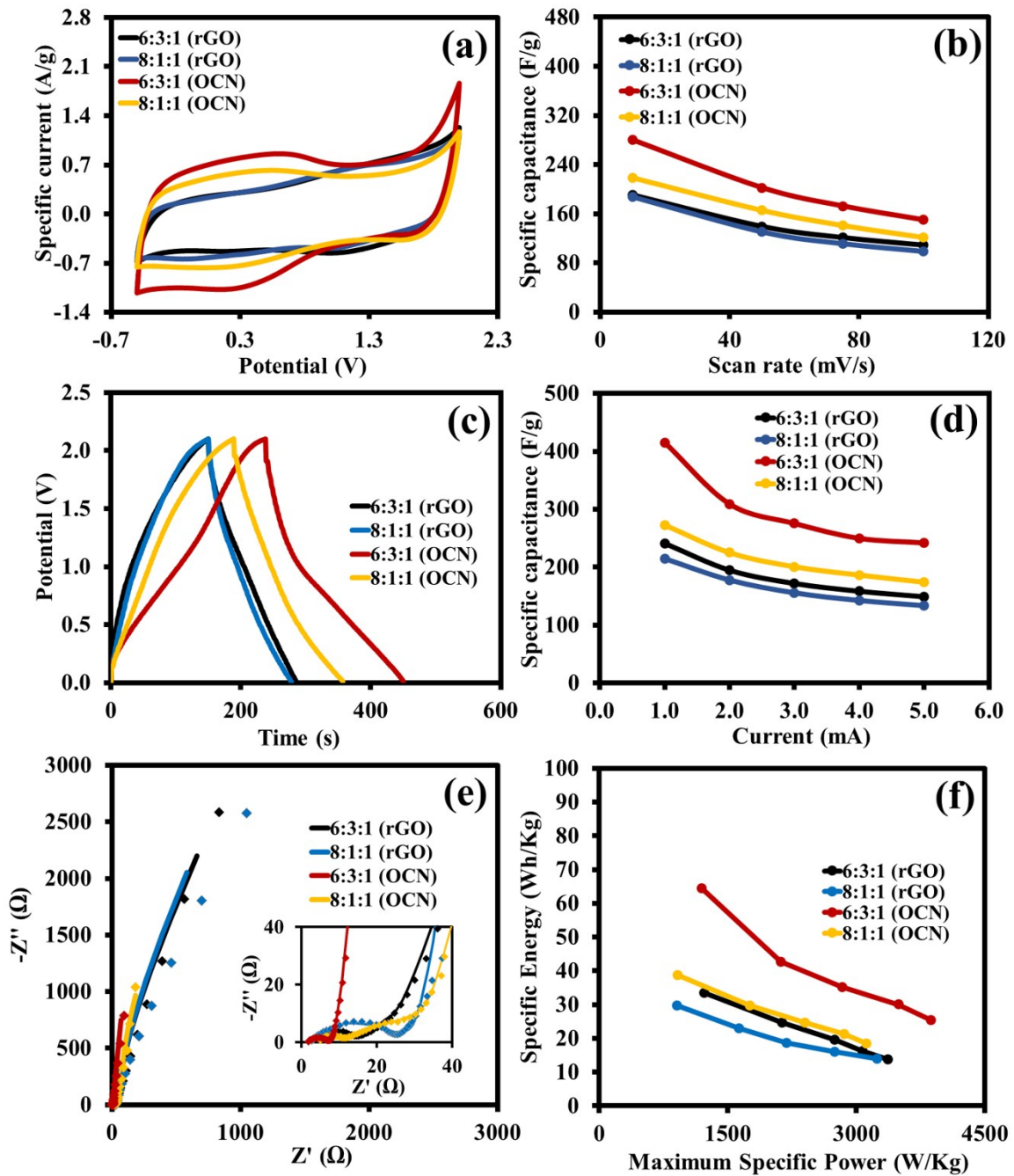


**Fig. S3.** (a) CVs at a scan rate of 10 mV/s, (b) the specific capacitances vs. the scan rates, (c) GCDs at an applied current of 2mA, (d) the specific capacitances vs. the applied currents, (e) Nyquist plots, and (f) Ragone plots of MnO<sub>2</sub>:OCN:PVDF and MnO<sub>2</sub>:rGO:PVDF supercapacitors at the weight ratios of 6:3:1 and 8:1:1.

Table S1. The charge storage performances of the MnO<sub>2</sub>-based supercapacitors

Materials	Electrolytes	Testing methods	Capacitances	Refs.
λ-MnO <sub>2</sub> :AC:PTFE on graphite sheet (7:2:1)	1.0 M Na <sub>2</sub> SO <sub>4</sub>	GCD 1 A/g	384 F/g	1
Graphene/MnO <sub>2</sub> /PEDOT	0.5 M Na <sub>2</sub> SO <sub>4</sub>	GCD at 0.1 mA/cm <sup>2</sup>	380 F/g	2
MnO <sub>2</sub> /CNTs:ACB:Conducting graphite:PTFE on a slice of carbon current collector (7.5:1:1:0.5)	1.0 M Na <sub>2</sub> SO <sub>4</sub>	GCD 1 A/g	201 F/g	3
N-doped graphene/MnO <sub>2</sub> :ACB:PVDF on Ni foam (8:1.5:0.5)	1.0 M Na <sub>2</sub> SO <sub>4</sub>	GCD 0.2 A/g	257.1 F/g	4
GO/MnO <sub>2</sub> :ACB:PTFE on Ni foam (7:1.5:0.5)	1.0 M Na <sub>2</sub> SO <sub>4</sub>	GCD at 150 mA/g	216.0 F/g	5
MnO <sub>2</sub> /CNTs/rGO:CB:PTFE on Ni foam (9:0.5:0.5)	1.0 M Na <sub>2</sub> SO <sub>4</sub>	GCD 0.2 A/g	193 F/g	6
MnO <sub>2</sub> :ACB:PTFE on a flat glass surface (7:1.5:0.5)	0.5 M K <sub>2</sub> SO <sub>4</sub>	CV at 5 mV/s	241 F/g	7
rGO/CNTs/MnO <sub>2</sub> :ACB:PVDF on graphite paper (8:1.5:0.5)	1 M Na <sub>2</sub> SO <sub>4</sub>	GCD 0.5 A/g	319 F/g	8
MnO <sub>2</sub> :ACB:PTFE on Ni foam (8.5:1.5:0.5)	1 M Na <sub>2</sub> SO <sub>4</sub>	CV at 2 mV/s	191 F/g	9
MnO <sub>2</sub> :ACB:PTFE on stainless steel (7:2:1)	0.5 M Na <sub>2</sub> SO <sub>4</sub>	CV at 5 mV/s	200 F/g	10
MnO <sub>2</sub> :ACB:PVDF on Ni foam (7:2:1)	0.5 M Na <sub>2</sub> SO <sub>4</sub>	CV at 2 mV/s	222 F/g	11
MnO <sub>2</sub> /OCN/PVDF on <i>f</i> -CFP (6:3:1)	0.5 M Na <sub>2</sub> SO <sub>4</sub>	CV at 10 mV/s	280 F/g	This work
		GCD at 0.35 A/g	414 F/g	
		EIS at 10 mHz	363 F/g	



## References

1. S. Nagamuthu, S. Vijayakumar and G. Muralidharan, *Industrial & Engineering Chemistry Research*, 2013, **52**, 18262-18268.
2. G. Yu, L. Hu, N. Liu, H. Wang, M. Vosgueritchian, Y. Yang, Y. Cui and Z. Bao, *Nano Lett*, 2011, **11**, 4438-4442.
3. L. Li, Z. A. Hu, N. An, Y. Y. Yang, Z. M. Li and H. Y. Wu, *The Journal of Physical Chemistry C*, 2014, **118**, 22865-22872.
4. S. Yang, X. Song, P. Zhang and L. Gao, *ACS applied materials & interfaces*, 2013, **5**, 3317-3322.
5. S. Chen, J. Zhu, X. Wu, Q. Han and X. Wang, *ACS Nano*, 2010, **4**, 2822-2830.
6. Z. Lei, F. Shi and L. Lu, *ACS applied materials & interfaces*, 2012, **4**, 1058-1064.
7. O. Ghodbane, J. L. Pascal and F. Favier, *ACS applied materials & interfaces*, 2009, **1**, 1130-1139.
8. H. Jiang, Y. Dai, Y. Hu, W. Chen and C. Li, *ACS Sustainable Chemistry & Engineering*, 2014, **2**, 70-74.
9. J. Zhou, L. Yu, M. Sun, S. Yang, F. Ye, J. He and Z. Hao, *Industrial & Engineering Chemistry Research*, 2013, **52**, 9586-9593.
10. Y.-T. Wang, A.-H. Lu, H.-L. Zhang and W.-C. Li, *The Journal of Physical Chemistry C*, 2011, **115**, 5413-5421.
11. P. Wang, Y.-J. Zhao, L.-X. Wen, J.-F. Chen and Z.-G. Lei, *Industrial & Engineering Chemistry Research*, 2014, **53**, 20116-20123.